Electronic Supplementary Material (ESI) for Physical Chemistry Chemical Physics.

Supplementary data

A. Selection of the value of the Hubbard term in the GGA+U description

For the choice of U, the method used in a previous study[50] has been employed. The U_{Zn} and U_{Sb} values are selected to have the best representation of the formation energy of the main binary oxides of the elements: ZnO in the $P6_3mc$ space group and Sb_2O_3 in the Pccn space group. The results are given in Table A. It is obvious that for Antimony, no Hubbard term is necessary since the enthalpy of formation of Sb_2O_3 is correctly reproduced. For U_{Zn}, we have selected a value of 5eV which gives the best representation of the enthalpy of formation of ZnO.

These Hubbard parameters have been used to optimize the crystal structure of ZnSb. The cell parameters (Table B) are improved by using GGA+U compared to GGA. The calculated gap (0.11eV) and even the energy of formation (-0.0492eV/at) are in better agreement with the experimental data than within the GGA.

Table A: Gap and formation energy calculated with different values of U_{Sb} or U_{Zn} for the ZnO ($P6_3mc$) and Sb_2O_3 (Pccn) phases compared to experimental data.

Phase	U_{Sb} or U_{Zn} (eV)	Gap (eV)	$\Delta_f E$ (eV/at)	Reference
Sb_2O_3	0	2.18	-1.5028	This work
	-	3.38	-1.4717	Expe.[51]
ZnO	0	0.73	-1.5799	This work
	1	0.87	-1.6231	This work
	2	1.01	-1.6680	This work
	3	1.15	-1.7149	This work
	4	1.30	-1.7640	This work
	5	1.44	-1.8164	This work
	6	1.61	-1.8722	This work
	7.5	1.83	-	DFT[52]
	-	3.2±0.1	-1.8137±0.0207	Expe.[53,54]

B. Influence of the XC functional on the calculated properties of pure ZnSb

Different DFT functionals (LDA, GGA, GGA+U, mBJ, SCAN) have been used to calculate the cell parameters, elastic constants, electronic band gap, hole effective mass and the formation energy of the ZnSb compound.

A. Details of the calculations

The elastic constants are calculated using the procedure implemented in VASP[55]. For these calculations, the cut-off energy is increased to 600eV and a displacement of 0.08Å for each atom is used to calculate the Hessian matrix.

For density of states calculations, the k-point mesh is increased up to 31*31*31 (4096 k-points in the irreducible part of the Brillouin) for the conventional cell and 7*7*7 (172 k-points) for a 2x2x2 supercell.

The effective mass of the holes, m^*_h, is estimated from band structure calculations applying equation (A) to the highest valence band. The mass of the holes depends on the direction in reciprocal space and describes an ellipsoid. For ZnSb, the main axes of this ellipsoid correspond to the axes of the crystal[56]. Then, different masses can be calculated from $m^*_{h,x}$, $m^*_{h,y}$ and $m^*_{h,z}$for DOS or conduction applications by the equations (B) and (C) respectively where g is the degeneracy factor of the band.

$$m_{h,\beta}^{*} = \frac{\hbar^2}{\frac{\partial^2 E}{\partial k_\beta^2}} \quad \text{(A)}$$

$$m_{h,DOS}^{*} = \sqrt[3]{g^2 m_{h,x}^{*} m_{h,y}^{*} m_{h,z}^{*}} \quad \text{(B)}$$

$$\frac{1}{m_{h,cond}^{*}} = \frac{1}{3}\left(\frac{1}{m_{h,x}^{*}} + \frac{1}{m_{h,y}^{*}} + \frac{1}{m_{h,z}^{*}}\right) \quad \text{(C)}$$

B. Results

The results of the calculations are compared to the literature in Table B, Table C and Table D. For comparison, the cell parameters are taken from the Pearson database[18]. The enthalpy of formation of ZnSb has been experimentally re-measured, the discussion about this particular quantity is given in Benigni *et al.*[57]. The band gap has been measured several times, but only optical measurements[58,59] are retained here (both measurements at 300K (0.48eV[59] and 0.50eV[58]) are in perfect agreement). Moreover, the band gap has also been measured[58] at 4.2K (0.61eV) and at 77K (0.59eV). Using these values, the evolution of the experimental band gap with the temperature can be fitted as:

$$E_g(T) = 0.615 - 3.793.10^{-4}T \quad \text{(D)}$$

Our calculated cell parameters are similar to those previously published. Classical behaviours are obtained for ZnSb: the LDA underestimates the cell parameters whereas the GGA overestimates them with respect to experiment. The best agreement is obtained for GGA+U and SCAN. As a consequence, the calculated elastic constants are highly overestimated in LDA and underestimated in GGA. The best agreement is obtained for SCAN since GGA+U does not reproduce the anisotropic behaviour of the elastic constants obtained with all the other functionals.

For the electronic band gap, LDA and GGA are dramatically unable to reproduce the experimental value (up to a factor 20 of underestimation). For the SCAN and GGA+U methods, even if the gap is better reproduced than in LDA or GGA, these functionals underestimate the gap by a factor close to 6. However, a combination of GGA or GGA+U with mBJ gives a perfect reproduction of the experimental gap.

The effective masses of the holes in ZnSb have been calculated with equation (1). Whatever the functional, the lowest masses are found in the z direction and the highest masses in the y direction which is consistent with previous calculations and with experimental measurements (Table C). The mean DOS effective masses have been calculated at around 0.14-0.16m_0. It is obvious that, if mBJ improves the value of the gap, mBJ also modifies the shape of the bands, resulting in higher values of the DOS effective masses: 0.230m_0 for GGA+mBJ and 0.256m_0 for GGA+U+mBJ. However, taking into consideration the high uncertainty in the experimental determination of the masses, the results on this quantity are not discriminant for this study.

Concerning the formation enthalpy, whatever the functional, the results are far from the experimental values (see Table B). If both LDA, SCAN and GGA highly underestimate $\Delta_f E$ (50% to 100% difference), HSE06 highly overestimates $\Delta_f E$ (in the same proportions depending on the experimental value selected). The best agreement is obtained with GGA+U.

Finally, no functional allows to represent all the parameters or properties correctly. However, an overall agreement is obtained for the GGA+U description (+mBJ for the electronic properties) and SCAN. Nevertheless, it is not possible to select un-ambiguously the best functional. Therefore, in the rest of this study, the GGA+U and SCAN descriptions will be used to calculate the thermoelectric properties of pure ZnSb.

Table B: Cell parameters, gap and formation energy calculated with different DFT methods for the ZnSb phase compared to literature

Method	Cell parameters (Å)			Gap (eV)		$\Delta_f E$ (eV/atom)	Reference
	a	b	c	Standard	mBJ		
LDA	6.1086	7.5817	7.9859	-	-	-0.002	3

	6.0981	7.5840	7.9870	0.05	-	+0.0044	This work
GGA	-	-	-	-	-	-0.04	60
	6.287	7.824	8.229	0.05	-	-	61
	6.2818	7.8246	8.2299	0.05	-	-0.0375	3
	6.286	7.812	8.232	0.05	-	-	14
	-	-	-	-	0.60	-0.027	13
	6.2839	7.8227	8.2246	0.03	0.61	-0.0316	This work
GGA+U	6.2536	7.8178	8.2028	0.11	0.65	-0.0492	This work
SCAN	6.1768	7.6798	8.0998	0.11		-0.0222	This work
Expe.	6.207	7.740	8.087	0.615 at 0K		-0.0632 to -0.0819	18, 57, 58

Table C: Elastic constants (in GPa) of orthorhombic ZnSb calculated with different functionals,

	LDA	GGA	GGA+U	SCAN	GGA[3]	GGA[63]	Expe 80K[62]	Expe 300K[62]
C_{11}	108.2	80.8	80.3	97.3	80.2	81.4	98.4	92.4
C_{22}	122.0	95.9	89.2	109.1	93.3	92.8	112.7	103
C_{33}	108.0	86.6	85.7	94.9	84.4	80.9	97.2	93.6
C_{12}	40.5	32.3	28.2	32.1	29.5	30.1	33.9	32.9
C_{23}	37.7	29.0	24.7	26.3	26	26.3	32.4	31.1
C_{13}	42.1	31.9	30.6	31.6	29	29.1	36.2	38.4
C_{44}	21.2	18.9	17.5	21.5	18.5	18.5	23.2	21.6
C_{55}	45.7	36.1	37.8	43.6	37.6	36.7	53.2	46.3
C_{66}	35.8	29.5	30.1	35.9	30.2	29.0	39.3	36

Table D: Hole effective masses (in m_0)

	$m_{h,x}$	$m_{h,y}$	$m_{h,z}$	$m_{h,DOS}$	$m_{h,cond}$
LDA	0.189	0.460	0.080	0.149	0.302
GGA	0.173	0.478	0.076	0.143	0.293
GGA+U	0.201	0.606	0.084	0.162	0.345
SCAN	0.179	0.478	0.085	0.154	0.308
GGA-mBJ	0.265	0.538	0.135	0.230	0.426
GGA+U-mBJ	0.298	0.616	0.151	0.256	0.481
LACO[64]	0.30	0.76	0.13	-	-
GGA[31]	0.181	0.491	0.084	-	-
Expe[65]	0.55	1.23	0.34	-	-
Expe – 273K[66]	0.42	0.69	0.26	0.42±0.15	-
Expe – 273K[31]	-	-	-	0.33 to 0.6	-

C. Ternary phase diagrams X-Sb-Zn where X is the doping element

For Si, Ge and Pb, the ternary system X-Sb-Zn is pretty simple since no binary or ternary phases are reported in the literature. The doped ZnSb phase will be in competition with a 3-phase region ZnSb + element + Zn. The calculated section of the ternary system at 0K is reported in Figure Aa.

For Sn, several binary Sb-Sn phases have been reported, however according to our DFT calculations within SCAN, no one is stable. A ternary compound Sb_2SnZn has been experimentally identified in the literature and has a calculated formation energy of -0.050 eV/atom. The Sn-doped ZnSb phase will be in competition with a 3-phase region ZnSb + Sb2SnZn + Zn. The calculated section of the ternary system at 0K is reported in Figure Ab.

For Ga and In, a binary phase XSb is reported. The calculated energy of formation in SCAN slightly underestimates the measured enthalpy of formation of GaSb (Table E). The doped ZnSb phase will be in competition with a 2-phase region ZnSb + XSb without zinc vacancy and with a 3-phase region ZnSb

+ XSb + Sb with zinc vacancies. The calculated section of the ternary system at 0K is reported in Figure A.c).

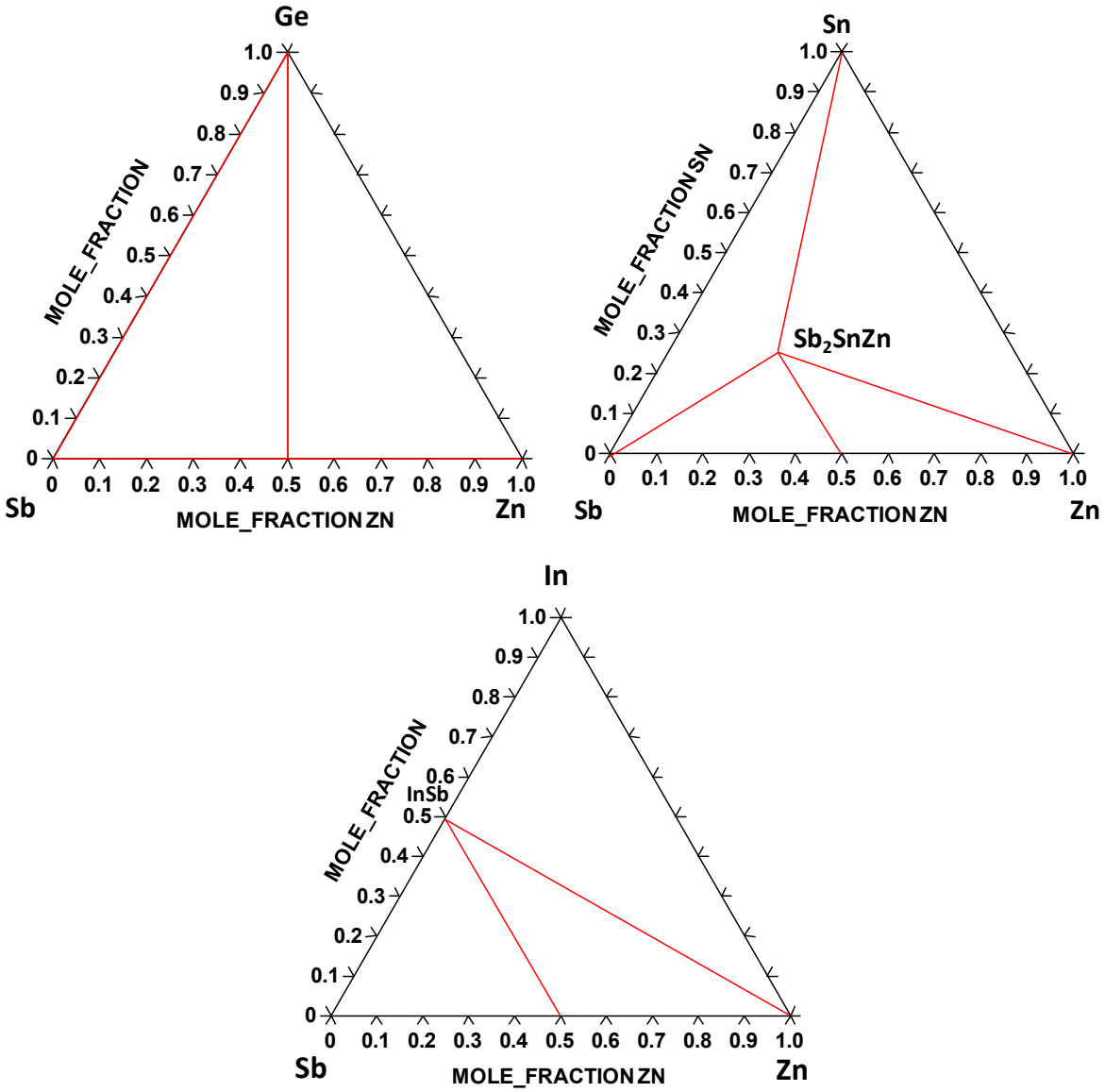

Figure A: ternary phase diagram X-Sb-Sn for X=: a) Ge, Si and Pb; b) Sn, c) Ga and In

Table E: Calculated formation energy of binary and ternary phases in the systems X-Sb-Zn compared to the experimental enthalpy of formation.

Phase	$\Delta_f E$ (eV/atom)	$\Delta_f H$ (eV/atom)
	SCAN	Experimental
GaSb	-0.163	-0.204 to -0.238[67]
InSb	-0.178	-0.155 to -0.168[67]
SnSb	-0.197	-
Sb2SnZn	-0.050	-

D. TE properties of ZnSb with one vacancy and several In_{Zn}

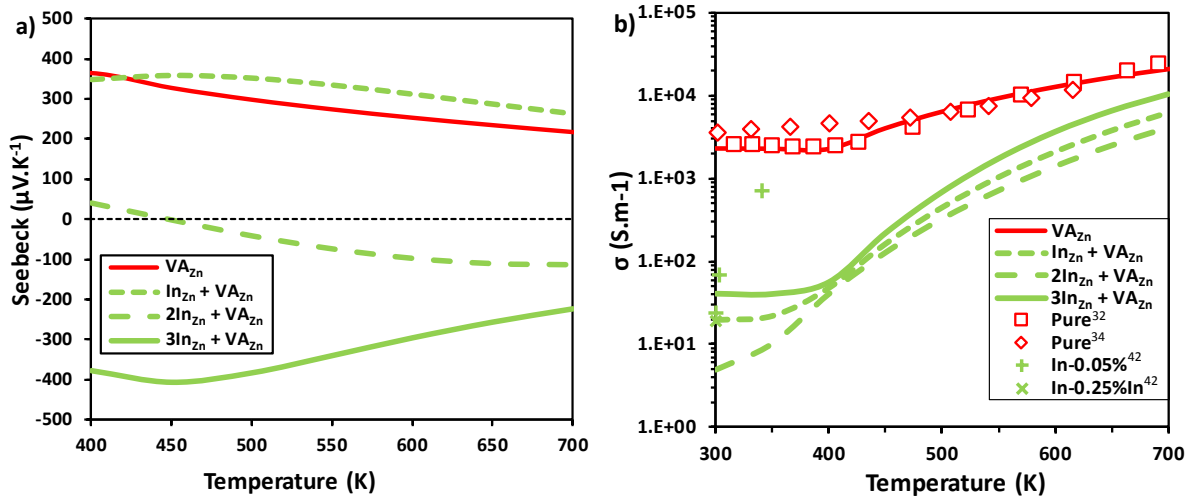

Figure B: Evolution of the Seebeck coefficient (a) and the electrical conductivity (b) as a function of temperature for 2x2x2 supercells containing one zinc vacancy plus zero (solid red), one (green dashed), two (green dot-dashed) or three (solid green) In_{Zn} compared to experimental values.

Additional references

50- A. Berche and P. Jund, *Intermetallics*, 2018, **92**, 62
51- M. Aspiala, D. Sukhomlinov, P. Taskien, *Solid State Ionics*, 2014, **265**, 80
52- P. Erhart, K. Albe and A. Klein, *Phys. Rev. B*, 2006, **73**, 205203
53- V. Srikant and D.R. Clarke, *J. Applied Phys.*, 1998, **83**(10), 5447
54- H.A. Wriedt, *Bull. Alloy Phase Diag.*, 1987, **8**(2), 166
55- R. Yu, J. Zhu and H. Ye, Comput. Phys. Commun., 2010, 181(3), 671
56- A.W. Carlson, Technical report NASA-CR-85579, 1967, SR-3
67- P. Benigni, A. Berche, R. Pothin, A. Adenot, G. Mikaelian, R.M. Ayral, P. Jund, J. Rogez, Calphad, 2017, 58, 204
58- H. Komiya, K. Masumoto and H.Y. Fan, *Phys. Rev. A*, 1964, **133**(6), 1679
59- M. Zavetova, *Phys. Status Solidi*, 1964, **5**, K19-K21
60- A.S. Mikhaylushkin, J. Nylén, U. Häussermann, *Chem. Eur. J.*, 2005, **11**, 4912
61- D. Benson, O.F. Sankey, U. Häussermann, *Phys. Rev. B*, 2011, **84**, 125211
62- N. Balazyuk, A.I. Eremenko, N.D. Raransky, *Funct. Mater.*, 2008, **15**, 343
63- P. Hermet, M.M. Koza, C. Ritter, C. Reibel, R. Viennois, *RSC Advances*, 2015, **5**, 87118
64- G.L. Zhao, F. Gao, D. Bagayoko, *AIP Advances*, 2018, **8**, 105211
65- A.W. Carlson, PhD. Thesis, Massaschussetts Inst. Tech. (Cambridge) 1967
66- P.J. Shaver and J. Blair, *Phys. Rev.*, 1966, **141**(2), 649
67- V.P. Vasil'ev and J.C. Gachon, *Inorg. Mater*, 2006, **42**(11), 1176